Scientific Research Publishing

Open Journal of Air Pollution, 2024, 13, 23-55
https://www.scirp.org/journal/ojap
ISSN Online: 2169-2661
ISSN Print: 2169-2653

Distribution of Atmospheric Pollution in Southern Benin

Dossou-Gbete Sèdami Codjo Joël[1], Kpadonou Dominique[2], Gbaguidi An Magloire[2], Elegbede Vitalique[1], Saizonou Kpèssou Virtus Mickael[2], Youssao Abdou Karim Alassane[2], Dovonon Firmin Léonce[2], Vodounnon Armand[3]

[1]Doctoral School of Exact and Applied Sciences, University of Abomey-Calavi (UAC), Abomey-Calavi, Benin
[2]Ecotoxicology and Quality Study Research Unit, Applied Chemistry Study and Research Laboratory, Department of Chemical Engineering-Processes (GC-P), Polytechnic School of Abomey-Calavi, University of Abomey-Calavi, Abomey-Calavi, Benin
[3]Africa Synergy Group Plus, Cotonou, Benin
Email: dominiquekpadonou8@gmail.com

How to cite this paper: Joël, D.-G.S.C., Dominique, K., Magloire, G.A., Vitalique, E., Mickael, S.K.V., Alassane, Y.A.K., Léonce, D.F. and Armand, V. (2024) Distribution of Atmospheric Pollution in Southern Benin. *Open Journal of Air Pollution*, **13**, 23-55.
https://doi.org/10.4236/ojap.2024.131002

Received: November 13, 2023
Accepted: March 26, 2024
Published: March 29, 2024

Abstract

This study focuses on air quality in southern Benin in order to show public authorities what the Beninese populations are exposed to for efficient decision-making. Two sampling campaigns were carried out, one in the wet period and the other in the dry season. The measurements were taken using a monitor called an "Air Quality Monitor". For data processing, the multiple comparison methods of Dun (1961) and the Wilcoxon test were used. To maintain legitimacy, all spatial data were included in the official cartographic repository of Benin: WGS 1984, Transverse Mercator Universe Projection (UTM), Zone 31 North. The Moran statistic was used to measure the levels of spatial autocorrelation of the variables studied and to test the significance. In order to locate the spatial subsets, the local spatial association indices of Anselin Local Moran and Getis-Ord, Gi* were used. In terms of results, on the 13 monitoring sites and the 8 parameters chosen to determine air quality, we do not note any significant inter-seasonal difference. Of the eight parameters, only three parameters present spatial autocorrelation leading to predictions of ambient air quality over the entire study area based on the distance separating the points, namely, $PM_{2.5}$, PM_{10} and ambient air quality index (AQI). The localities affected by atmospheric pollution in South Benin are located in the south-western part of Benin, headed by Cotonou, which is heavily polluted by CO_2, TCOV, PM_{10} and $PM_{2.5}$.

Keywords

Spatial Distribution, Atmospheric Pollutants, Southern Benin

1. Introduction

Air pollution is a problem that has raised awareness since the start of the industrial era in 1848, and became more visible at the end of the 19th century [1]. Just like water and soil, air quality is of paramount importance for most living beings, especially aerobic ones [2]. Like other parts of the world, Africa is increasingly affected by air pollution in its major cities. According to the World Health Organization (WHO) estimate in 2012, 11.6% of deaths worldwide were linked to indoor and outdoor air pollution. This represents nearly 6.5 million deaths per year, 3 million of which are attributable solely to ambient air pollution [3]. The largest share of these deaths (88%) occurred in low- and middle-income countries [4] [5] [6]. Thus, the assessment of exposure to air pollution and its health and environmental impacts now constitutes a major and priority challenge in disadvantaged countries [3]. Thus, in Benin, law no. 2019-40 of November 7, 2019 revising Law No. 90-32 of December 11, 1990 establishing the Constitution of the Republic of Benin elevates environmental protection to constitutional status. Article 27 stipulates that "every person has the right to a healthy, satisfactory and sustainable environment and has the duty to defend it. The State therefore ensures the protection of the environment." This constitutional provision is accompanied by several regulatory texts including Law No. 98-030 of February 12, 1999 on the framework law on the environment in the Republic of Benin and Decree No. 2001-110 of April 4, 2001 on quality standards of air in the Republic of Benin still in force. Outside of the regulatory framework, we have the establishment of several institutions including the Ministry of Living Environment and Transport (MCVT) with its specialized structures such as the Beninese Environment Agency (ABE), the General Directorate of Environment and Climate (DGEC) and its decentralized and deconcentrated services which are supposed to facilitate the practical implementation of policies environmental measures designed and developed by the umbrella structures. So, faced with air pollution in large cities, Benin has adopted several initial studies, a national strategy to combat air pollution serving as a master plan to conduct operations to combat this scourge [7]. Despite this panoply of institutional and legal provisions and the efforts made by the various governments to protect the environment, the living environment in Benin continues to be degraded due to poverty, incivility, ignorance and illiteracy [8] [9]. This study was initiated in order to show public authorities what the Beninese populations are exposed to when making decisions in this direction.

2. Materials and Methods

2.1. Study Zone

Figure 1 shows the map of the sampling sites.

2.2. Methodology for Measuring Concentrations of Atmospheric Pollutants for Monitoring Air Quality

Before the measurement campaigns took place, a prospective visit was carried

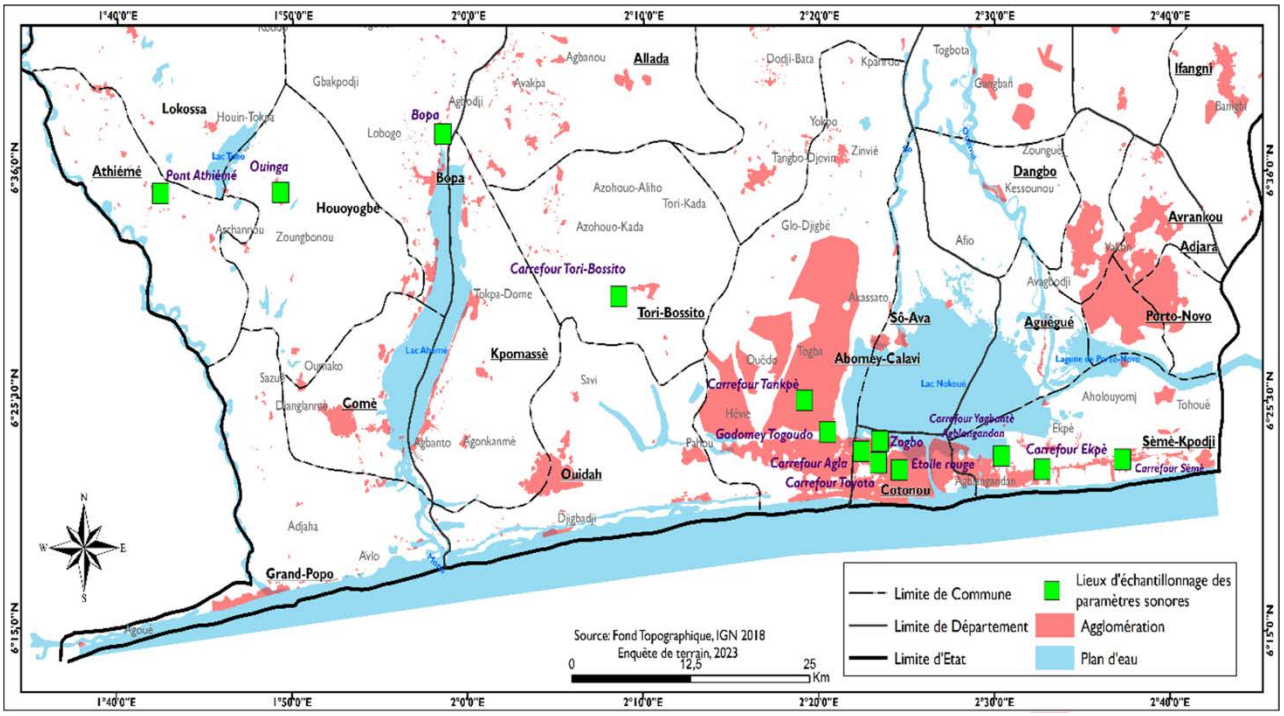

Figure 1. Mapping of the zonation of sampling sites in southern Benin (Source: This study).

out on the road sections during which 13 sites were identified for monitoring including 9 hot spots and 4 points in the background areas. Table 1 presents the list of ten (13) measurement sites, their location and their characteristics (heavy traffic lane paved or not).

Air quality measurements were taken using autonomous electronic devices called "Air Quality Monitor", powered by a lithium battery or by connection to the mains, via a transformer. The device is calibrated for 4 hours at first start-up in ambient air. Once switched on, the measuring device automatically determines the concentrations of carbon dioxide CO_2, Total Organic Compounds (TVOC), methanal (CH_2O), particulate matter with diameters of 2.5 µm and 10 µm denoted PM2, 5 and PM_{10}, temperature in degrees Fahrenheit (˚F = 1˚C × 1.8 + 32) and the hygrometry (Relative humidity H%) of the ambient air. Recordings were carried out for an entire day at each measurement site in 30-minute intervals. Measurements generally start at 7 a.m. and end at 6 p.m. with 24 measurements per site. In Cases of delay, the measurement is extended beyond 6 p.m. to compensate for the delay. Units of measurement are parts per million air particles (ppm) or micrograms per cubic meter. These different parameters provide information, alone or combined, on the quality of ambient air.

2.3. Processing of Recorded Data

The processing methods cover all the operations applied to the data to bring them as close as possible to the nominal terrain. These are descriptive statistics techniques which make it possible to achieve inferential statistics and spatial type processing.

Table 1. Ambient air quality measurement sites in southern Benin.

Codes	Names of air quality measurement sites	Geographic coordinates
S1	Carrefour Sèmè-Kpodji	N: 06˚22'86" E: 02˚37'23"
S2	Carrefour Ekpè	N: 06˚22'37" E: 02˚32'75"
S3	Carrefour Yagbantè (Aglangandan)	N: 06˚22'96" E: 02˚30'39"
S4	Von du Delegate Zogbo	N: 06˚23'65" E: 02˚23'50"
S5	Carrefour Togoudo (Godomey)	N: 06˚24'03" E: 02˚20'49"
S6	Carrefour Tankpè (Calavi)	N: 06˚25'45" E: 02˚19'22"
S7	Bypass intersection (Tori Bossito)	N: 06˚30'14" E: 02˚08'57"
S8	Houègboh (Bopa)	N: 06˚38'00" E: 01˚58'47"
S9	Wangbo village Davè (Ouinga)	N: 06˚35'44" E: 01˚49'28"
S10	Athiémé border bridge	N: 06˚34'02" E: 01˚39'52"
S11	Red Star Crossroads	N: 06˚22'17" E: 02˚24'35"
S12	Carrefour Cica Toyota	N: 06˚22'37" E: 02˚23'23"
S13	Carrefour Agla-Friendship Stadium	N: 06˚23'28" E: 02˚23'09"

Source: This study.

In this research [10], multiple comparison method was used. The Wilcoxon test was used to determine the existence of a significant difference in the temporal evolution of the concentrations of the pollutants measured, at the different sampling points. Concerning the geometric transformation, it consisted of registering all the georeferenced data in the same projection system. To maintain legitimacy, all spatial data were included in the official cartographic repository of Benin: WGS 1984, Transverse Mercator Universe Projection (UTM), Zone 31 North. The Moran statistic was used to measure the levels of spatial autocorrela-

tion of the variables studied and to test the significance.

2.4. Measuring Global Spatial Dependence

The Moran statistic [11] is the spatial autocorrelation index used. It allows you to measure the level of spatial autocorrelation of a variable and to test its significance. It is equal to the ratio of the covariance between contiguous observations, defined by the spatial interaction matrix, to the total variance of the sample. The index has values between-1 (indicating perfect dispersion) to 1 (perfect correlation). A zero value means that the spatial distribution of the variable studied is perfectly random in the territory. Negative (positive) values of the index indicate negative (positive) spatial autocorrelation. An interpretation of the Moran index is given as follows:

- In the presence of spatial autocorrelation, we observe that the value of a variable for one observation is linked to the values of this same variable for neighboring observations.
- Spatial autocorrelation is positive when similar values of the variable being studied cluster together geographically.
- Spatial autocorrelation is negative when dissimilar values of the variable to be studied are grouped together geographically: close places are more different than distant places. This type of situation is generally found in the presence of spatial competition.
- In the absence of spatial autocorrelation, we can consider that the spatial distribution of observations is random.

Figure 2 gives an interpretation of the p-value and the z-score when processing spatial data.

2.5. Measuring Local Spatial Dependence

In order to locate the spatial subsets, the local spatial association indices of Anselin Local Moran and Getis-Ord, Gi*, are used:

- **Getis and Ord index**

Getis and Ord [12] propose an indicator (Gi) making it possible to detect local spatial dependencies which do not appear in the global analysis. Thus, the Gi* from Getis-Ord makes it possible to analyze concentrations (hot pot). An interpretation of the values of this indicator is given as follows:

Gi > 0 indicates a grouping of values higher than average.

Gi < 0 indicates a grouping of values lower than the average.

- **Local Anselin Moran index**

Anselin [13] develops the notions introduced by Getis and Ord by defining local spatial autocorrelation indicators (Ii). These must make it possible to measure the intensity and significance of the local dependence between the value of a variable in a spatial unit and the values of this same variable in the surrounding spatial units. More precisely, these indicators make it possible to detect significant groupings of identical values around a particular location (aggregate)

and to identify areas of spatial non-stationarity, which do not follow the overall process.

Ii > 0 indicates a grouping of similar values (higher or lower than average).

Ii < 0 indicates a grouping of dissimilar values (e.g. high values surrounded by low values).

2.6. Assessment of Air Quality

To assess air quality, we used Table 2 which presents the guide values for assessing

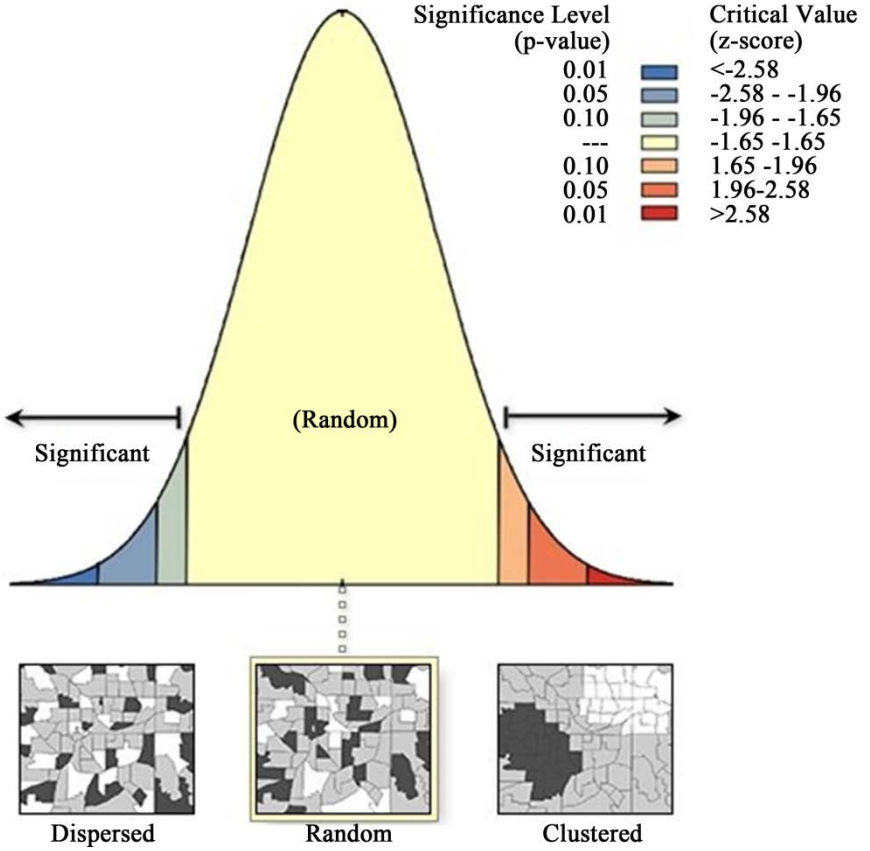

Figure 2. Guide values of p-value and Z-score for decision-making (Source: This study).

Table 2. Guide values for assessing air quality

Air quality	Carbon dioxide (CO_2) in ppm	TVOC (mg/m³)	HCHO (mg/m³)	Fine particles ($PM_{2.5}$) in µg/m³	Particulate matter (PM_{10}) in µg/m³	AQI
Good	400 - 600	0 - 0.3	0 - 0.1	0 - 50	0 - 54	0 - 50
Moderate	651 - 1500	0.3 - 1.0		16 - 40	55 - 154	51 - 100
Unhealty for sensitive group	1501 - 2000	1.0 - 3.0		41 - 65	155 - 254	101 - 150
Unhealty	2001 - 2500	3.0 - 10.0	>0.1 mg/m³	66 - 150	255 - 354	151 - 200
Very unhealty	2501 - 5000	>10.0		151 - 250	355 - 424	201 - 300
Hazardous	5001 - 15000			251 - 500	425 - 604	301 - 500

Source: This study.

air quality based on the limit values of the World Health Organization (WHO) and regulations, Beninese. These values are defined by the manufacturer of the mobile air pollutant measurement monitor.

3. Results and Discussion

3.1. Case of Temperature

The map in Figure 3 shows the spatial variability of temperature in southern Benin.

From the analysis of Figure 3, we note that the temperatures vary from 20˚F to 95˚F with an average of 69.5˚F ± 21˚F and a %CV = 30. Therefore, the values taken by the temperature are dispersed over the study zone. The standard deviation ellipse is oriented East-West. We deduce from this the existence of a direction in the distribution of temperature values. This allows us to suspect a spatial dependence of ambient temperature values, hence the need to test spatial autocorrelation. Moran's Spatial Autocorrelation Index = 0.489992 at the 0.03 threshold. This index is different from 0, which leads us to say that the realization of the regionalized random variable is therefore dependent. It is therefore possible to predict the temperature values at one point, knowing the values observed at another point, based on the distance that separates them. This observed dependence may be the result of chance. It is therefore necessary to verify the validity of this spatial dependence on a global scale. This statistical test of independence of the regionalized variable carried out is General G which gives a Z score equal to 0.711827 and a p-value of 0.476572 greater than alpha = 0.05. This test puts the interpretation of the spatial autocorrelation test into perspective and allows us to conclude that the hypothesis of spatial dependence is not verified and is only the effect of chance.

3.2. Case of Relative Humidity RH

Figure 4 shows the spatial distribution of the values taken by the relative humidity RH.

Analysis of the map in Figure 4 reveals, as in the Case of the temperature map, that the standard deviation ellipse is oriented West-East, raising suspicion of a direction in the spatial distribution of relative humidity data. which suggests a spatial dependence of the humidity data.

The spatial autocorrelation index gives a value = −0.382090 at the threshold of 0.298181 greater than alpha. Therefore, there is no autocorrelation between relative humidity values on a global scale. However, carrying out the General G test gives an index of 0.000023 read at the threshold of 0.37. It confirms the interpretation of the Moran index and allows us to conclude on the non-existence of aggregates in which local autocorrelation is expressed.

3.3. Case of CO_2

The map in Figure 5 shows the spatio-temporal variation of CO_2 levels. From

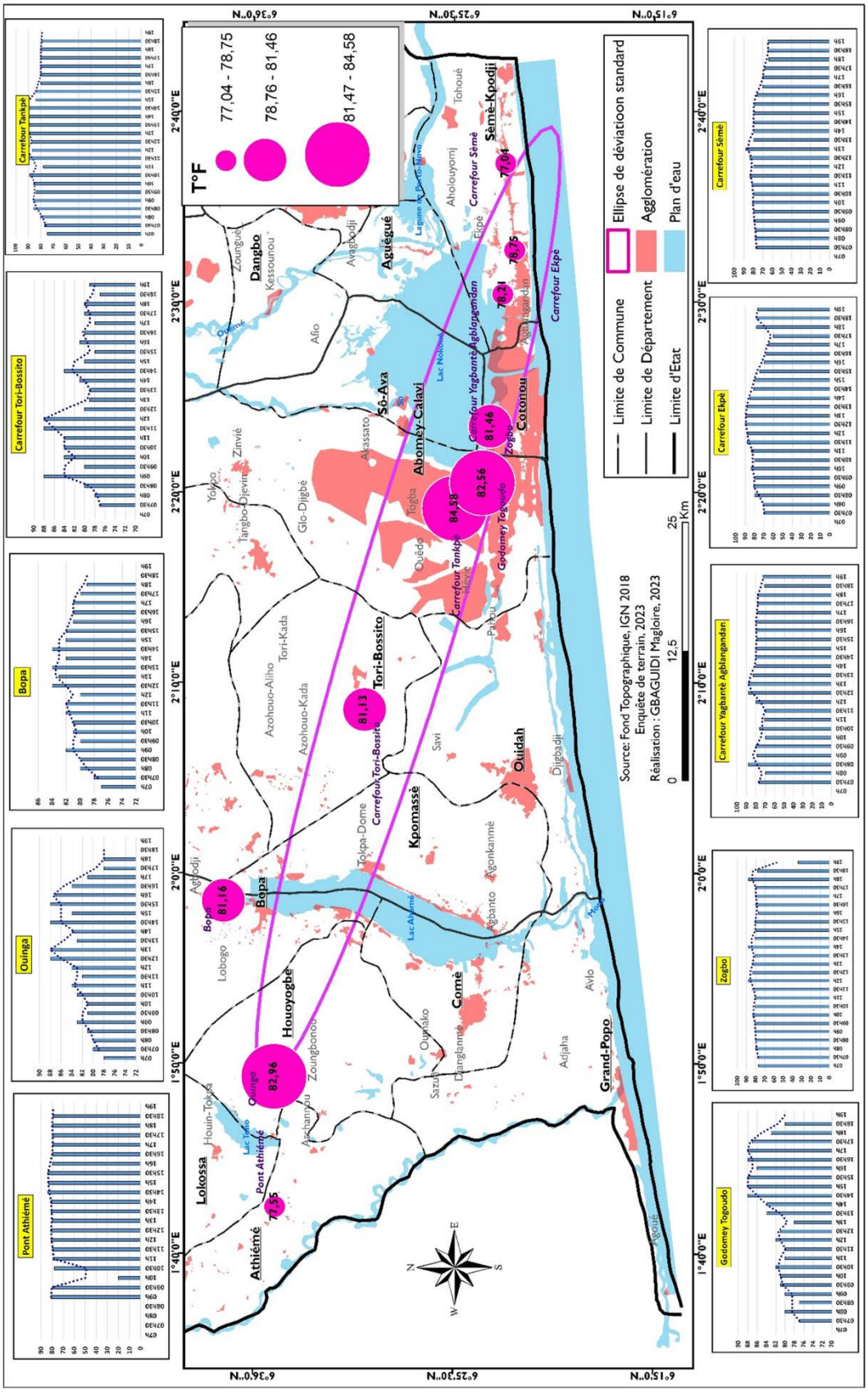

Figure 3. Spatial distribution of temperature (Source: This study).

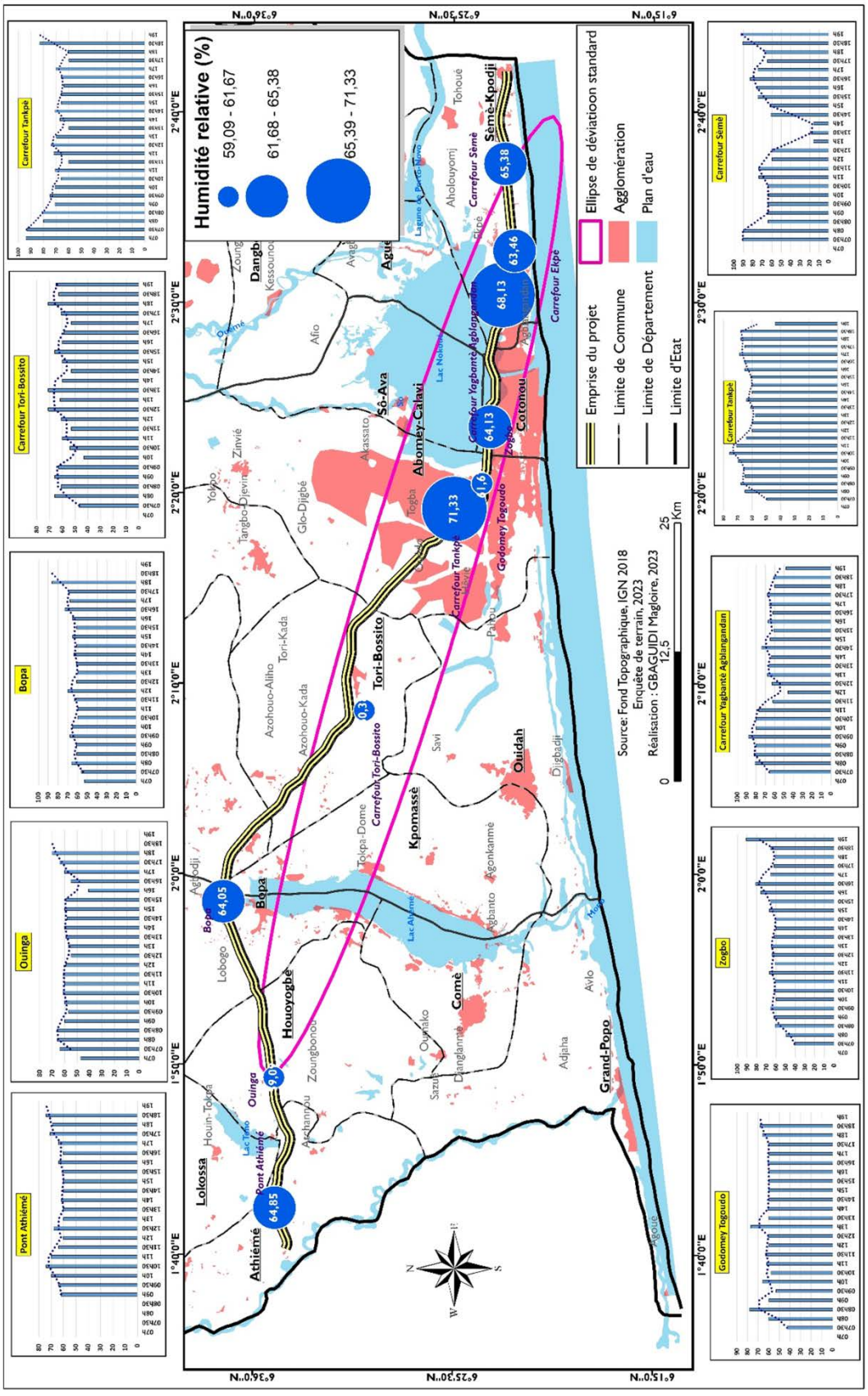

Figure 4. Spatial distribution of relative humidity RH in southern Benin (Source: This study).

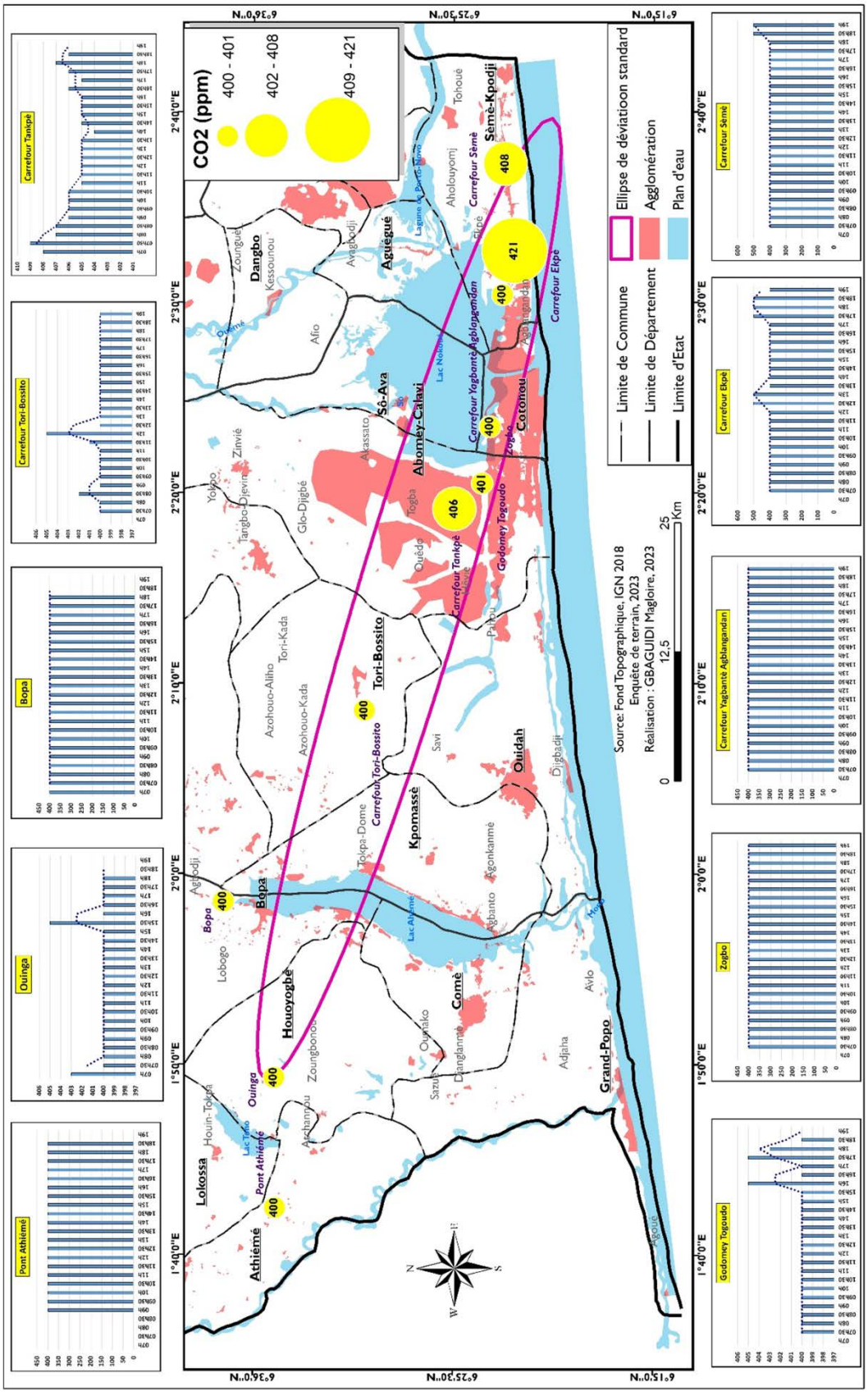

Figure 5. Spatial distribution of CO_2 levels in southern Benin (Source: This study).

the analysis of the map data, it appears that the CO_2 contents vary between 400 and 1444 ppm with an average of 486.8 ± 184.33 ppm and a %CV = 37.86. CO_2 levels vary from one site to another. The high CO_2 emission zones are located at the major intersections of Cotonou such as the "Etoile rouge, Sica Toyota and Terrain" intersections.

The calculation of the spatial autocorrelation index carried out on the 10 collection points and the values observed on these points present the following results: Moran's spatial autocorrelation index = −0.13; p-value = 0.91. The Moran index is close to 0. The realization of the regionalized random variable is therefore independent. This means that the CO_2 values at a collection point are not influenced by the values observed in neighboring points. It is therefore not possible to predict the CO_2 values at one point, knowing the values observed at another point, based on the distance that separates them. This observed independence may be the result of chance and only has value for the sample used for the calculation. It is therefore necessary to carry out a test to verify the validity of this spatial independence for the spatial variable in its entirety. This statistical test of independence of the regionalized variable gives a Z score equal to −0.10 at the threshold of 0.91. This threshold is below the critical threshold of 5%. We deduce from this a total absence of spatial autocorrelation over the entire variable. Given the z score of −0.10, the model does not appear to be significantly different from chance which supports the interpretation of the Moran index.

3.4. Case of $PM_{2.5}$

The map in **Figure 6** shows the spatial distribution of $PM_{2.5}$ values.

From the analysis of the information from the map in **Figure 6**, we note that the standard deviation ellipse is oriented East-West leading to suspect a spatial dependence of the $PM_{2.5}$ pollution data.

The Moran index is different from 0 at the threshold of 0.012211. There is therefore a probability of less than 5% that this clustered pattern is the result of chance. To confirm or refute this trend, we searched for the General G index whose z-score is 3.06427722821, hence there is less than 1% probability that this highly clustered pattern is the result of chance. To confirm or refute this trend, we looked for the General G index whose value is 0.000049 read at the threshold of 0.002. Exploring this test at the local scale reveals the existence of aggregates in which local autocorrelation is expressed. It is therefore appropriate to identify these aggregates and look for the factors behind these concentrations of similar values at certain points. In order to locate these spatial subsets, the local spatial association indices of Anselin Local Moran and Gi* of Getis-Ord are used.

The calculation of the Anselin and Moran Local Index is carried out on the values taken by $PM_{2.5}$ in order to identify areas of similarity. **Figure 7** and **Figure 8** show the maps relating to the levels of similarity/dissimilarity between neighboring points and highlight areas with homogeneous or heterogeneous values.

The map in **Figure 7** shows that we have categorized where the Anselin Local

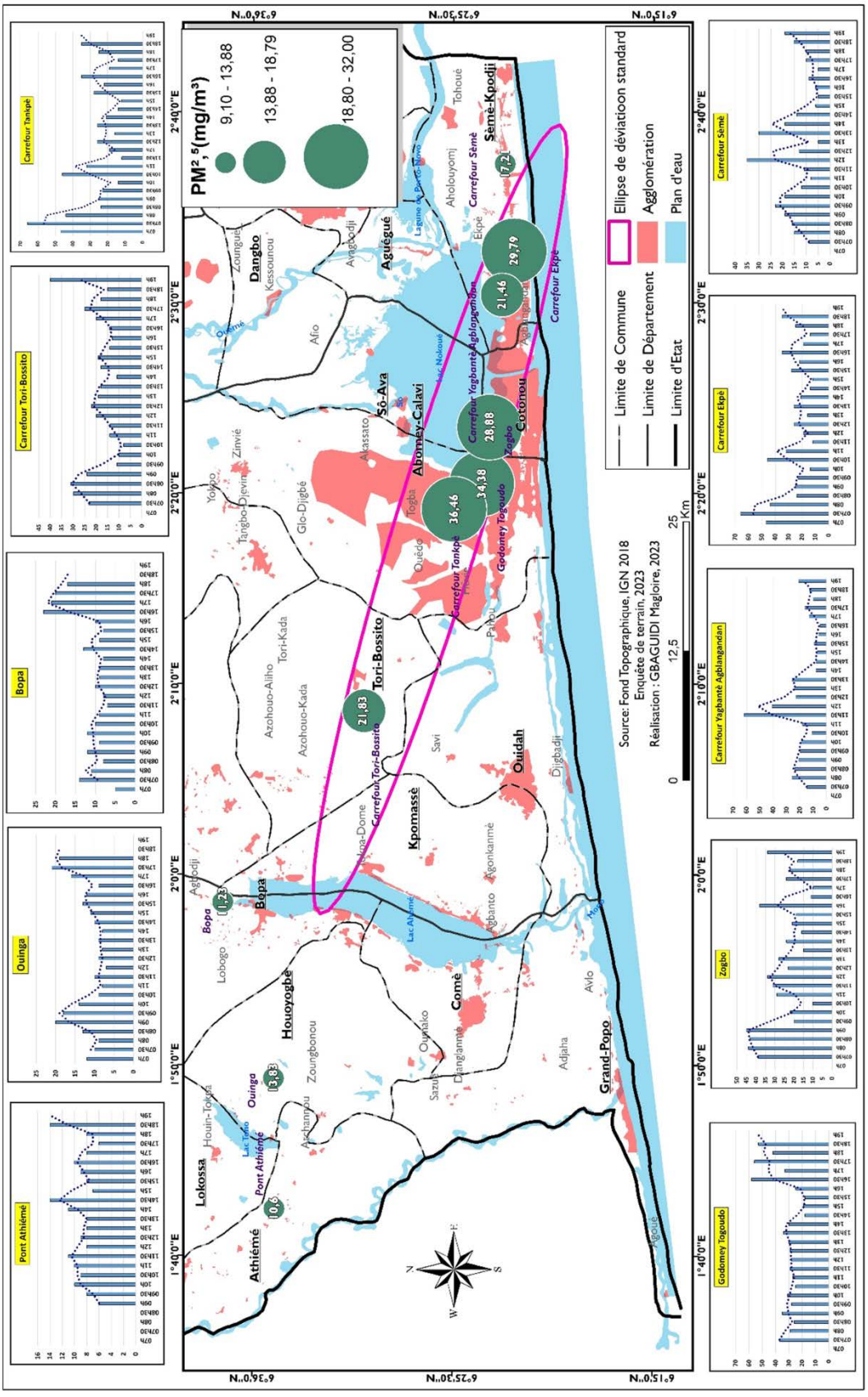

Figure 6. Spatial distribution of $PM_{2.5}$ concentrations in southern Benin (Source: This study).

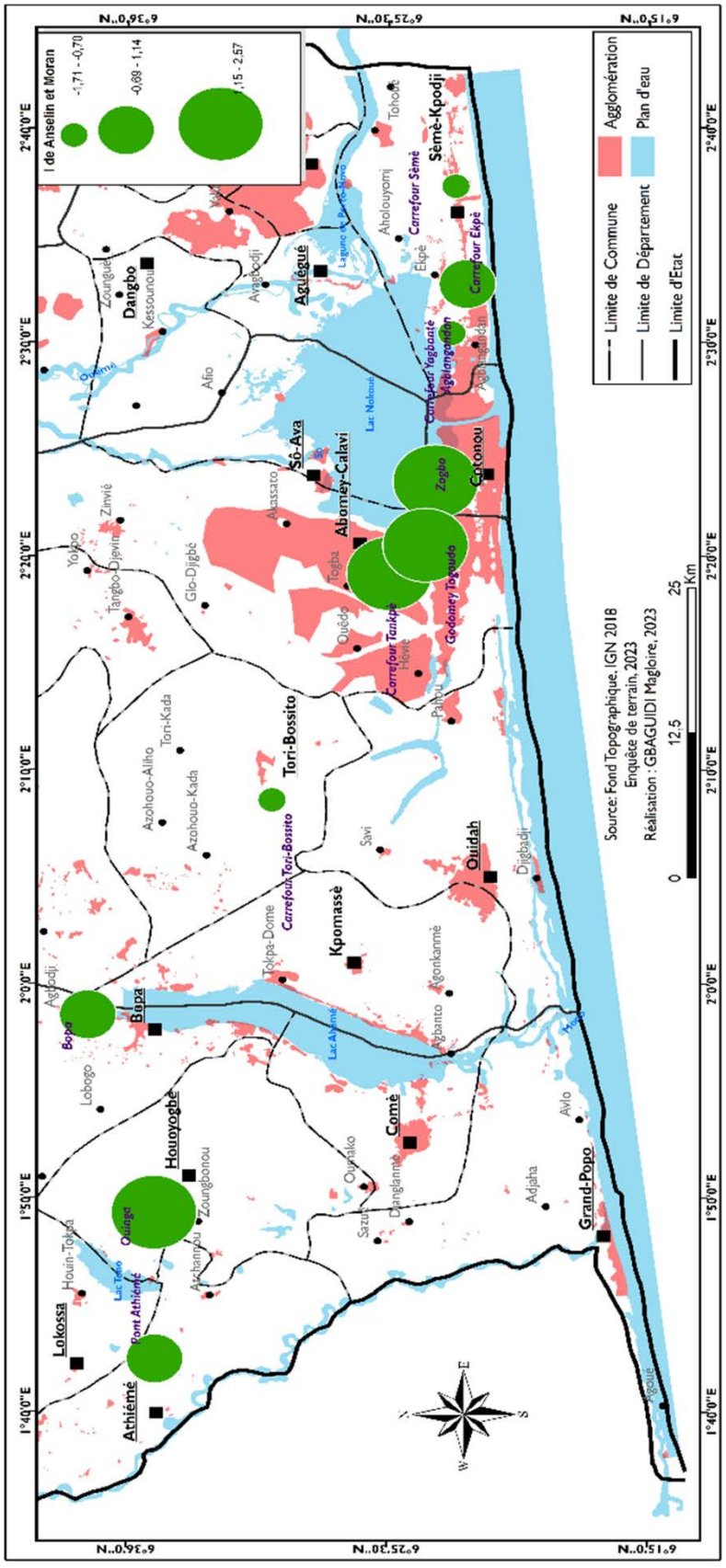

Figure 7. Areas of similarity in $PM_{2.5}$ content in the study area (Source: This study).

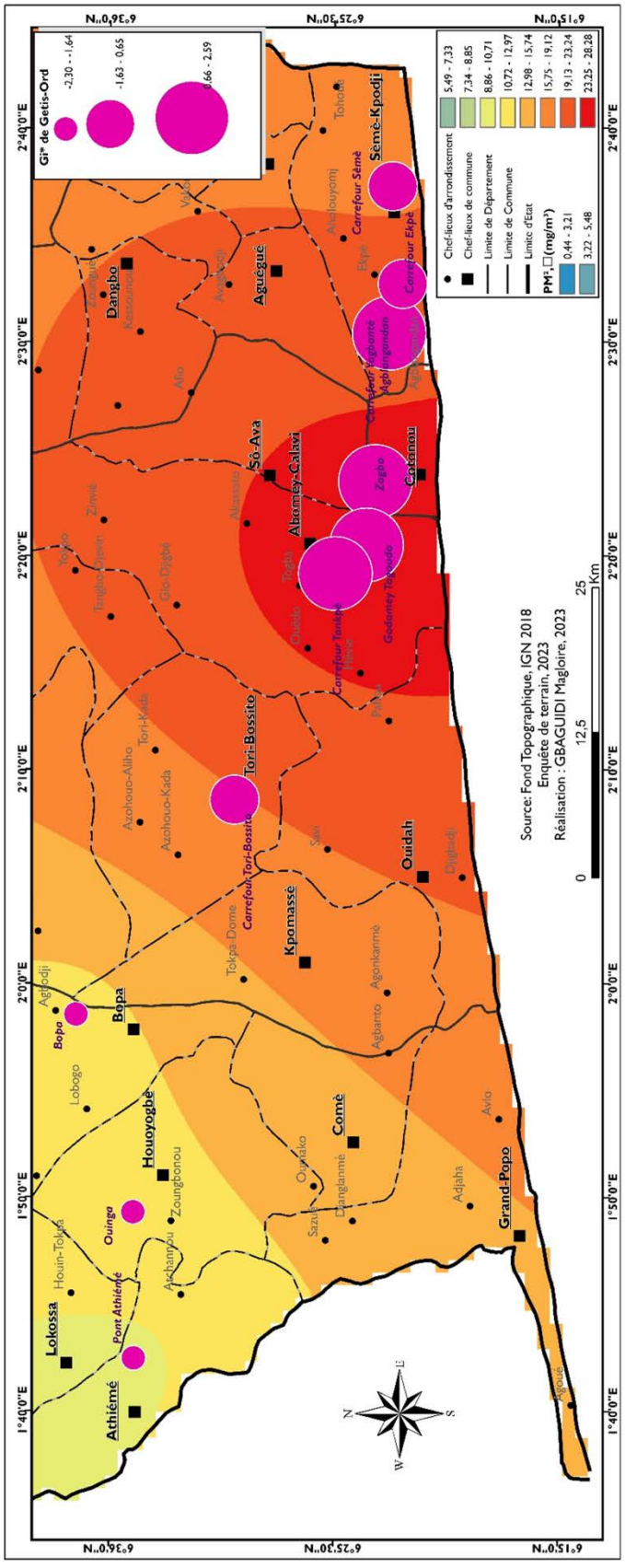

Figure 8. Spatial evolution of $PM_{2.5}$ levels in southern Benin (Source: This study).

Moran Index Z score values have been categorized into three classes. The low value class (−1.71 to −0.70) expresses a dissimilarity between neighboring points. The classes of average values (−0.69 to 1.14) expressing an average similarity and high values (1.15 - 2.57) giving the strong similarities between neighboring points. Analysis of the map information in Figure 7 reveals two clusters of points in the southwest and one cluster of points in the southeast. The first cluster in the southwest is a subset of points of low similarity and medium similarity. On the other hand, the 2nd subset brings together points of strong similarity. The last subset is composed of medium and strong similarity points. The first subset and the 3rd subset are therefore heterogeneous zones, which implies that the $PM_{2.5}$ values observed in these places are dissimilar. The hypothesis of the existence of a structure in the spatial distribution of $PM_{2.5}$ values is therefore verified. However, it is necessary to analyze the aggregates more closely. This is what the use of the Getis-Ord GI* index aims to achieve.

In order to identify areas of high concentration (hot pot) and areas of low concentrations of $PM_{2.5}$, we used the Gi* from Getis-Ord. Map 30 shows the spatial distribution of hot pot areas. The Getis-Ord GI* Z score presents the following statistics in the dry season for the 18 observation points: the minimum Z score is −1.83, its maximum 1.70 for an average of 0.64 and a standard deviation of 1.18; the accumulation of all the values being 22.98.

From the analysis of the map in Figure 8 it appears that high exposures to $PM_{2.5}$ are concentrated in the southwest of Benin and more precisely in the city of Cotonou and its surroundings and the further one moves away from Cotonou going towards the East, $PM_{2.5}$ pollution decreases. The least polluted area of the study area is the south-eastern part of Benin.

3.5. Case of PM_{10}

The map in Figure 9 shows the spatial distribution of PM_{10} levels in southern Benin. From the analysis of this Figure, we see that the direction ellipse is stretched on the East/West axis. It covers 6 observation points out of 13, or 46.15% of the PM_{10} values observed. We deduce the existence of a direction in the distribution of PM_{10} values. This allows us to suspect a spatial dependence of PM_{10} values, hence the need to test spatial autocorrelation.

Data analysis reveals that the Moran index is different 0 at the threshold 0.000336 andthe z-score is 3.58581379254, hence, there is less than 1% probability that this clustered pattern is the result of chance. The General G index gives 0.000065 at the threshold of 0.000061 with a z-scoreof 4.00809924822. General G's statistic confirms that of Moran, that is to say that there is less than 1% probability that this highly grouped model is the result of chance.It is therefore appropriate to identify these aggregates and look for the factors behind these concentrations of similar values at certain points. In order to locate these spatial subsets, the local spatial association indices of Anselin Local Moran and Gi* of Getis-Ord are used. The calculation of the Anselin and Moran Local Index is

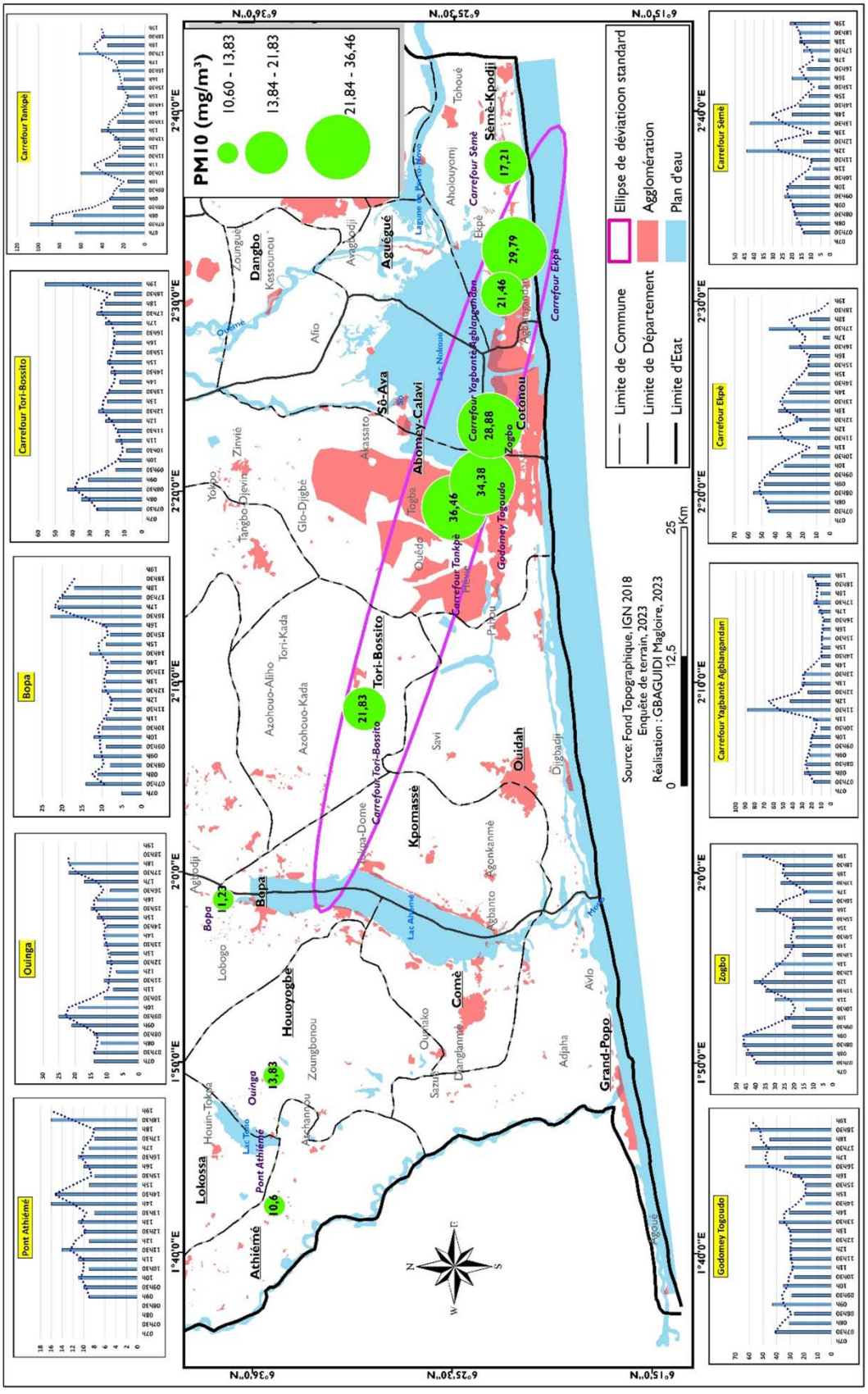

Figure 9. Spatial distribution of PM_{10} levels (Source: This study).

carried out on the values taken by PM_{10} in order to identify areas of similarity. Figure 10 and Figure 11 show the levels of similarity/dissimilarity between neighboring points and highlight areas with homogeneous or heterogeneous values.

The map in Figure 10 shows three classes of Z score values of the Anselin Local Moran index. The low value class (−1.47 to −0.12) expresses a dissimilarity between neighboring points. The classes of average values (−0.11 to 1.29) expressing an average similarity and high values (1.30 - 2.54) giving the strong similarities between neighboring points. Analysis of the information on map 32 reveals two clusters of points in the southwest and one cluster of points in the southeast. The first cluster in the southwest is a subset of low similarity points. On the other hand, the 2nd subset brings together points of strong similarity. The last subset is composed of medium and strong similarity points. This area is therefore heterogeneous, which implies that the PM_{10} values observed in this location are dissimilar. The hypothesis of the existence of a structure in the spatial distribution of PM_{10} values is therefore verified. This observed distribution is therefore not the result of chance. However, it is necessary to analyze the aggregates more closely. This is what the use of the Getis-Ord GI* index aims to achieve.

In order to identify areas of high concentration (hot pot) and areas of low concentrations of PM_{10}, we used the Gi* from Getis-Ord. The map in Figure 11 presents the spatial distribution of hot pot zones obtained from the classification of Z GI* scores into three classes at the natural Jenks threshold and spatialization.

From the analysis of Figure 11, we note that the area of high pollution by PM_{10} is the city of Cotonou and Abomey-Calavi.

3.6. Case of TCOV

The TCOV in the study area ranges from 0.01 to 6.91 mg/m^3 with an average of 0.35 ± 0.65 mg/m^3 and %CV = 181.38. From these remarks we can conclude that the values are dispersed around the average. The spatial distribution of TCOV contents is presented in Figure 12. From the analysis of this Figure, it appears that the standard deviation ellipse is oriented in the East-West axis, from where we deduce the existence of a direction in the distribution of TCOV values. This allows us to suspect a spatial dependence of the values of Total Volatile Organic Pollutants (TCOV), hence the need to test the spatial autocorrelation of the levels of this parameter.

From the analysis of the data, it appears that the Moran index is close to 0 at the threshold of 0.787762. So we deduce a total absence of spatial autocorrelation of TCOV contents. This total absence of autocorrelation may be the result of chance or due to the size of the sample used. To remove the doubt, we calculated the General G index which gives 0.000031 at the threshold of 0.110337 greater than alpha = 0.05. This statistic definitively confirms the trend observed with Moran's statics and we can safely say that there is a total absence of autocorrelation

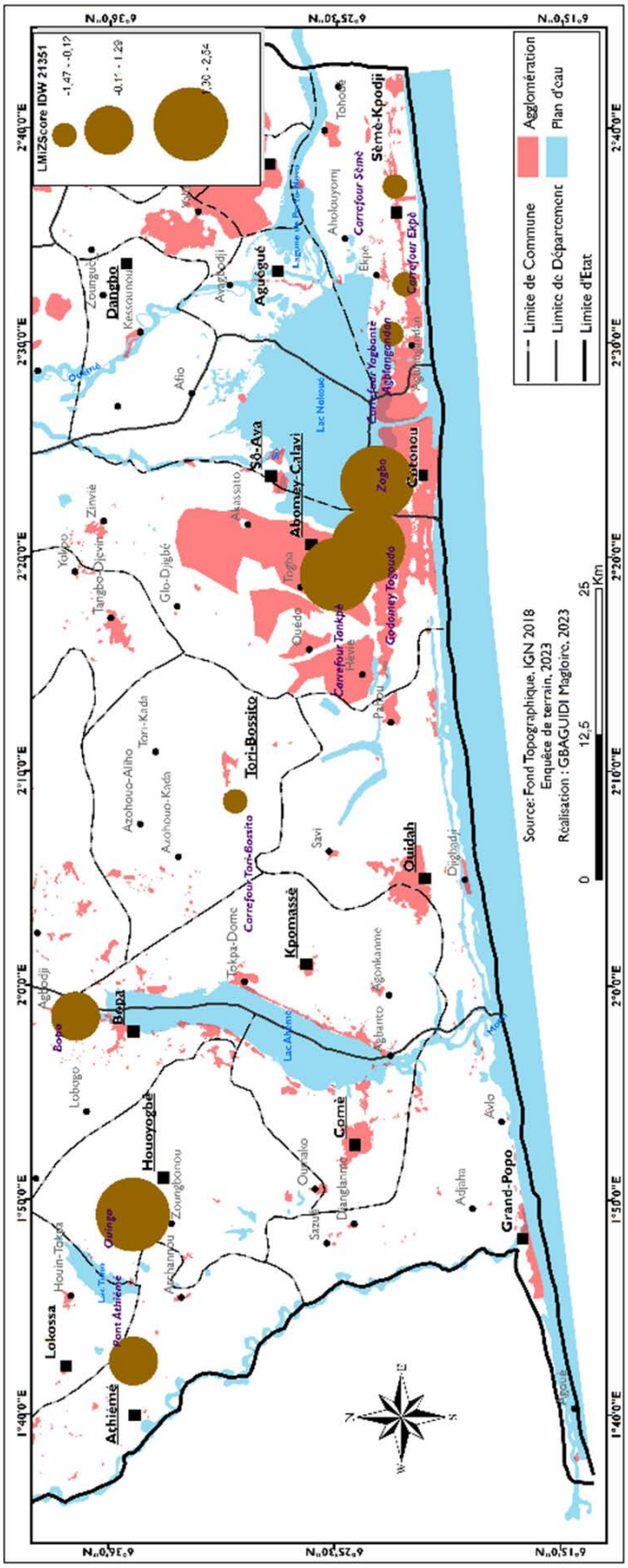

Figure 10. The areas of similarity and dissimilarity of values taken by PM_{10} (Source: This study).

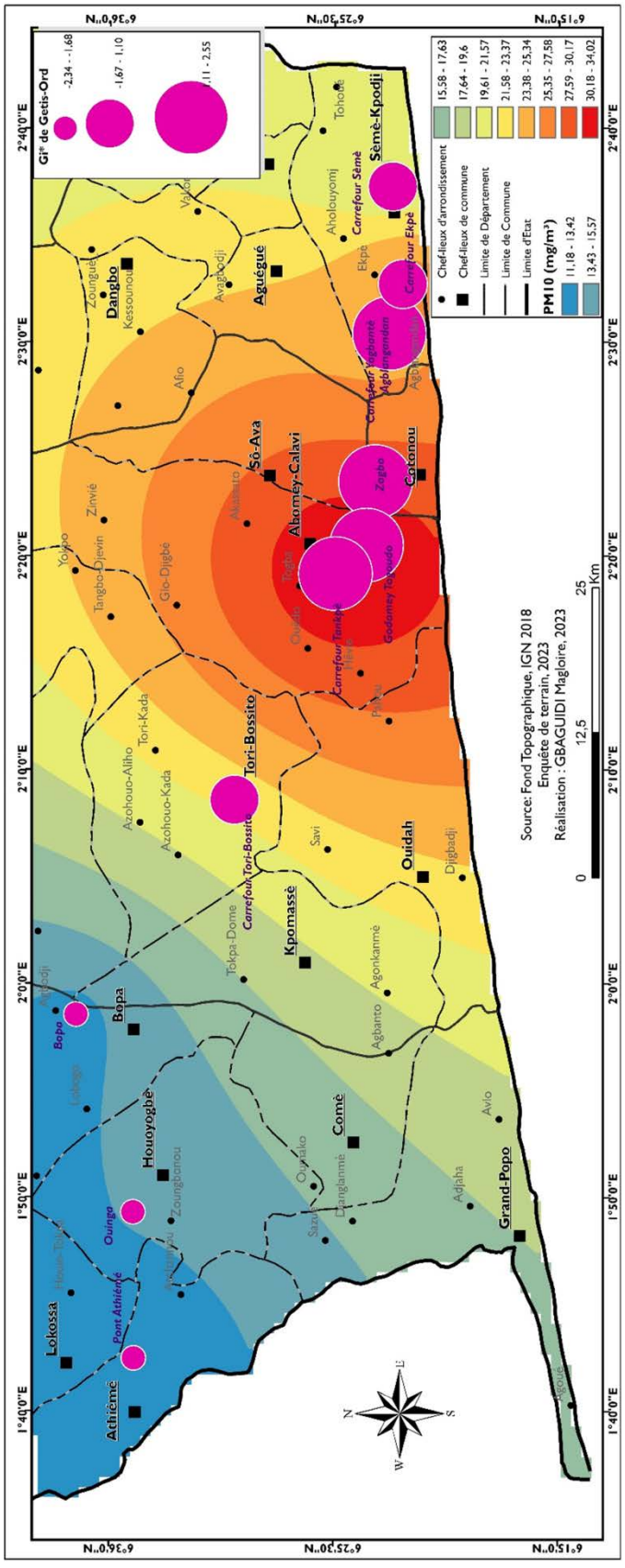

Figure 11. PM_{10} pollution hot pot zones (Source: This study).

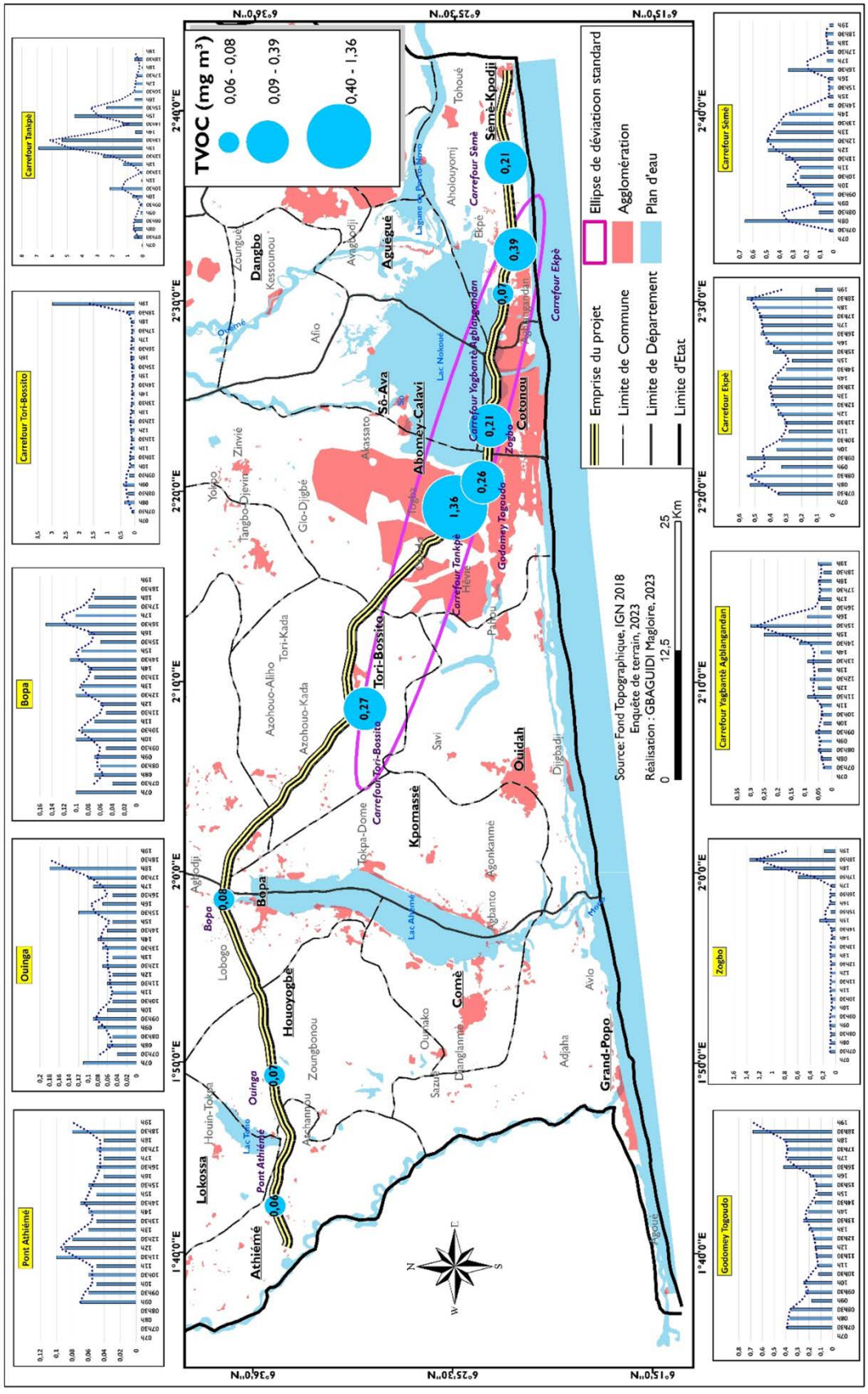

Figure 12. Distribution of TCOV contents (Source: This study).

in TCOV contents.

3.7. Case of Formaldehyde

HCHO contamination levels vary from 0.005 to 3 mg/m^3 with an average of 0.054 ± 0.17.62 mg/m^3 and a %CV = 320.90. The spatial distribution of aldehyde contents in the study area is presented by the map in **Figure 13**. From the analysis of this Figure, it appears that the standard deviation ellipse is stretched in the East-West direction. Then, the existence of a direction in the distribution of HCHO values can be considered and in turn suspect a spatial dependence of HCHO values, hence the need to test the spatial autocorrelation of the contents of this parameter.

From the analysis of the data, we note that the Moran index is close to O at the threshold of 0.218310 hence the absence of spatial autocorrelation of HCHO contents. This absence of spatial autocorrelation may be the result of chance or linked to the size of the sample used for the calculations. To remove the ambiguity, we calculated the General G index which gives 0.000031 and a p-value of 0.372789 greater than alpha. This statistic definitively removes the doubt and we can safely affirm that there is no spatial autocorrelation between the data observed for HCHO.

3.8. Case of the Air Quality Index (AQI)

From the analysis of the information recorded on the map in **Figure 14**, we can note that the AQI values vary from 03 to 243 with an average of 39 ± 31.16 and a coefficient of variation of 85.06. The standard deviation ellipse follows an East-West direction which suggests an orientation in the spatial distribution of the values taken by the Air Quality Index (AQI) and by extension suspect an autocorrelation in the distribution of the values of the AQI.

Analysis of the data shows that the Moran index is close to 0 at the threshold 0.068299 greater than alpha = 0.05 therefore, there is no spatial autocorrelation between the values taken by the AQI. This absence of spatial autocorrelation may be the result of chance and/or linked to the size of the sample used for the calculations, hence the need to verify this observation by calculating the General G index which gives 0.000060 at the threshold of 0.003085. This statistic puts the finding of the Moran index into perspective and highlights the existence at the local level of an autocorrelation between the values taken by the AQI.It is therefore appropriate to identify these aggregates and look for the factors behind these concentrations of similar values at certain points. In order to locate these spatial subsets, the local spatial association indices of Anselin Local Moran and Gi* of Getis-Ord are used. The calculation of the Anselin and Moran Local Index is carried out on the values taken by the Air Quality Index (AQI) in order to identify areas of similarity. **Figure 15** and **Figure 16** show the levels of similarity/dissimilarity between neighboring points and highlight areas with homogeneous or heterogeneous values.

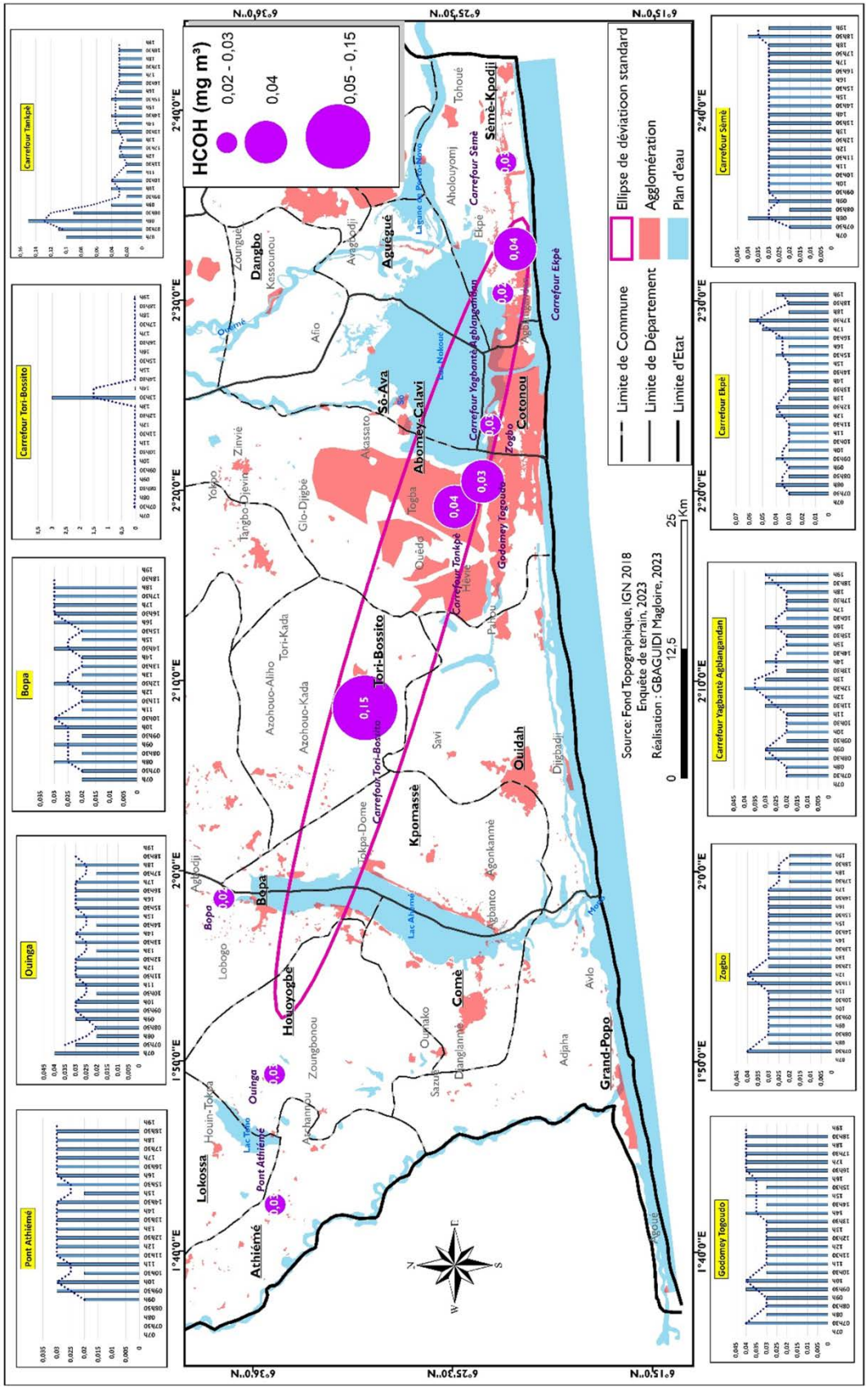

Figure 13. Spatial distribution of HCHO contents (Source: This study).

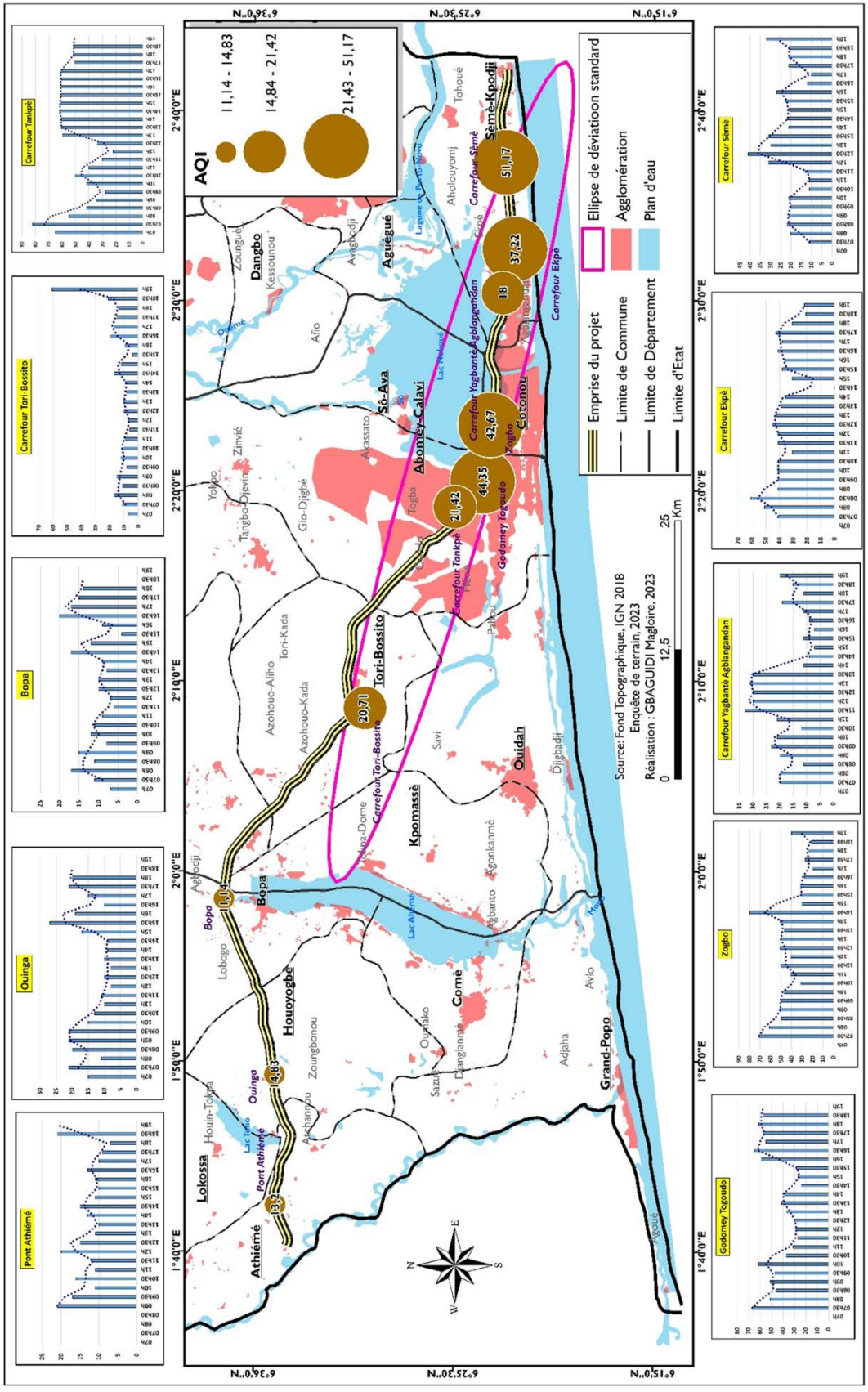

Figure 14. Spatial distribution of the values taken by the AQI (Source: This study).

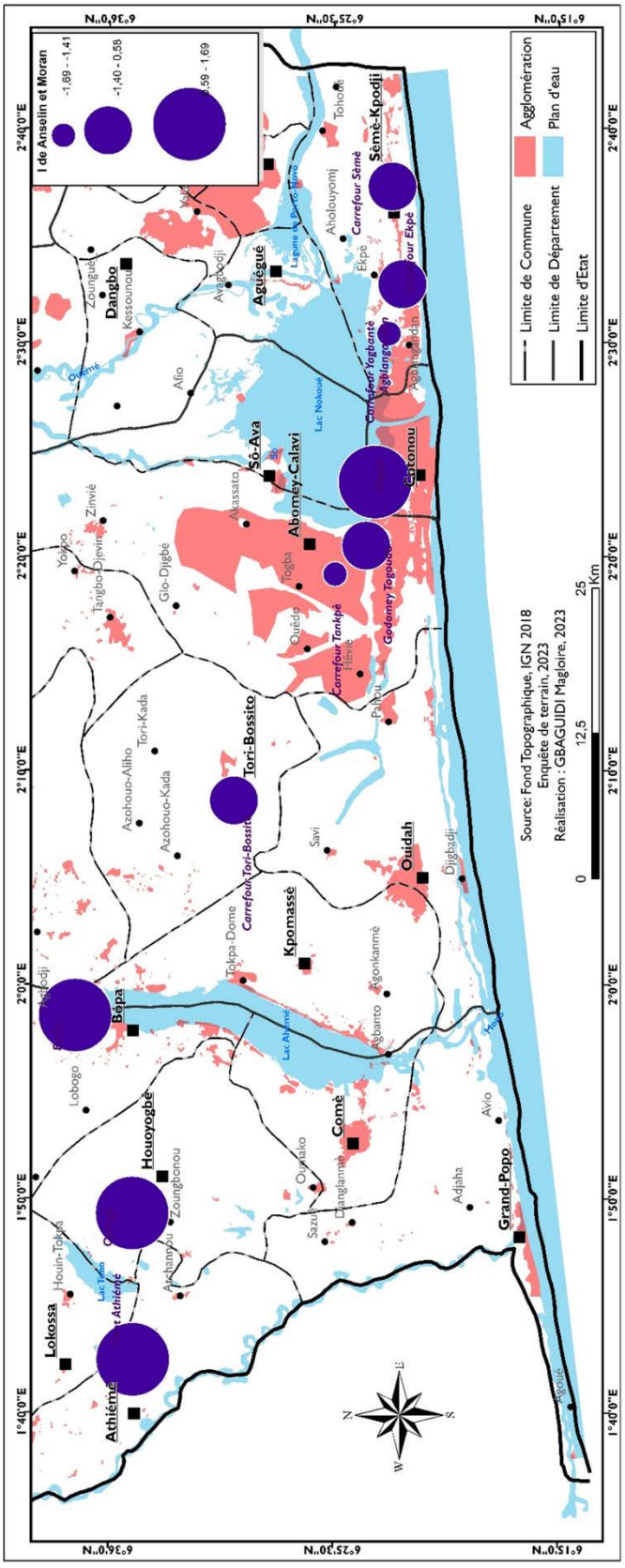

Figure 15. The areas of similarity/dissimilarity of the values taken by the AQI (Source: This study).

The map in Figure 15 shows three classes of Z score values of the Anselin Local Moran index. The low value class (−1.69 to −1.41) expresses a dissimilarity between neighboring points. The classes of medium values (−0.40 to 0.58) expressing an average similarity and high values (0.59 to 1.89) giving the strong similarities between neighboring points. Analysis of the information from map 15 reveals two clusters of points overall in the study area. The first cluster is a subset of points of low similarity and medium similarity. This area located in the southwest is therefore heterogeneous, which implies that the Air Quality Index (AQI) values observed in this area are dissimilar. On the other hand, the 2nd subset located in the southeast brings together points of strong similarity. The hypothesis of the existence of a structure in the spatial distribution of AQI values is therefore verified. There are concentration aggregates of strong and weak values as well as an orientation in the spatial distribution of AQI values. This observed distribution is therefore not the result of chance. However, it is necessary to analyze the aggregates more closely. This is what the use of the Getis-Ord GI* index aims to achieve.

In order to identify areas of high concentration (hot pot) and areas of low AQI values, we used Getis-Ord's Gi*. Map III.14 presents the spatial distribution of hot pot zones obtained from the classification of Z GI* scores into three classes at the natural Jenks threshold and spatialization.

From the analysis of the information on the map in Figure 16, it appears that the air quality index decreases from West to East, indicating that air quality is more degraded in the West than to the East.

3.9. Research of Key Parameters Influencing Air Quality on Each of the Sites Monitored

In this research, Principal Component Analysis was used to identify the different existing links between air quality monitoring parameters on the one hand and between air quality monitoring parameters on the other hand, air and tracking points. The correlation matrix in Table 3 reveals how the monitored parameters are correlated.

From the analysis of the information in Table 3, it appears that CO_2 is positively correlated with relative humidity at the 5% threshold. Thus, in conditions of high relative humidity, exposure to CO_2 becomes more significant with its corollaries of tearing headaches and suffocation in humans. This absence of links between the CO_2 levels and the levels of other ambient air quality monitoring parameters in southern Benin leads to the conclusion that the sources of CO_2 input into the ambient air at the measurement sites are not not exclusively road traffic. TCOV are significantly correlated with PM_{10}, temperature and the Air Quality Index at the 1% threshold and with $PM_{2.5}$ at the 5% threshold. In other words, the unburnt products coming out of chimneys and/or exhaust pipes impact the ambient air temperature due to their very high emission temperature. Likewise, these volatile organic compounds can be emitted in particulate form and/or adsorbed on inorganic particles which they coat. Aldehydes are not

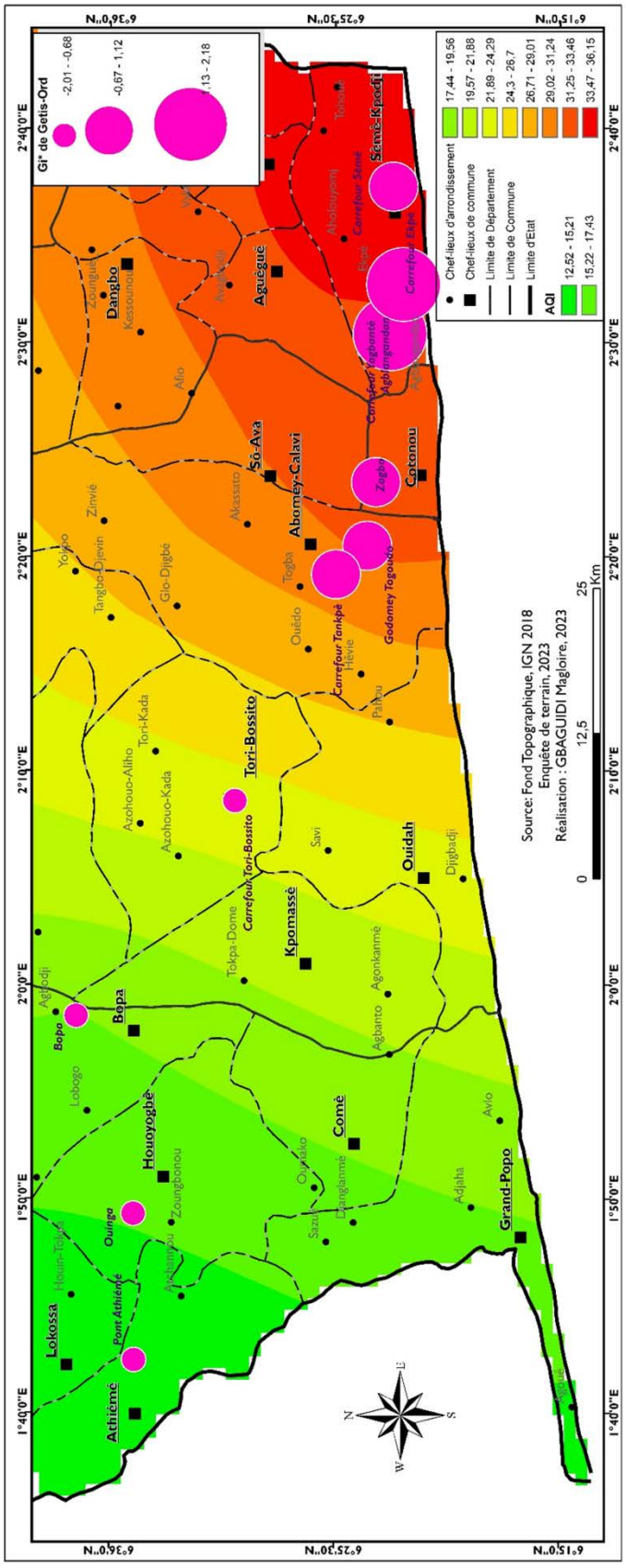

Figure 16. Spatial distribution of high and low AQI values (Source: This study).

Table 3. Correlation matrix.

	CO_2	TVOC	HCOH	$PM_{2.5}$	PM_{10}	T˚F	Humidity relative	AQI
CO_2	1							
TVOC	0.054	1						
HCOH	–0.005	–0.011	1					
$PM_{2.5}$	0.041	0.141*	0.017	1				
PM_{10}	0.073	0.211**	0.016	0.878**	1			
T˚F	–0.128	0.213**	–0.018	0.036	0.004	1		
Relative humidity	0.152*	0.048	0.053	0.070	0.098	–0.209**	1	
AQI	0.111	0.377**	0.000	0.670**	0.705**	0.129*	0.044	1

*Significant correlation at the 5% threshold; **Significant correlation at the 1% threshold.

Table 4. Eigenvalues and percentages of variances expressed by the principal axes.

	Val propre	% Total variance	Cumulative %
F1	2646	33,078	33,078
F2	1362	17,019	50,097
F3	1048	13,105	63,201
F4	1002	12,522	75,723

correlated with any of our ambient air quality monitoring parameters. This observation leads us to assume that aldehydes and TVOCs do not have the same emission sources. In other words, the aldehydes detected in the study presence, unlike TCOV which have a pyrolytic source, would come from other non-pyrolytic sources such as forests, industrial oxygenated organic solvents and others. **Table 4** presents the weights of the axes in the interpretation of the results of the Principal Component Analysis (PCA).

From the analysis of the data in this table, it appears that the first axis alone allows more than 33% of the information to be interpreted, while axis 2 only allows access to 17.02% of the information. The cumulative percentage gives for the first two axes a cumulative percentage of more than 50% interpretation of the analyzed data. By using the three axes we have access to more than 63% of the information compared to 75.7% using the first four axes, which is more than sufficient in the Case of our study. **Figures 17-19** present the graphical representations of the factor maps.

From the analysis of the information in **Figure 17**, we note that the AQI, $PM_{2.5}$ and PM_{10} are well represented on axis 1, while CO_2, relative humidity and temperature are carried by the axis 2. On this axis the temperature is diametrically opposite to relative humidity and CO_2.At the level of **Figure 17**, as at the level of **Figure 18**, axis 3 carries the temperature and TCOV.

In **Figure 19**, we note that the aldehydes are mainly carried by axis 4.

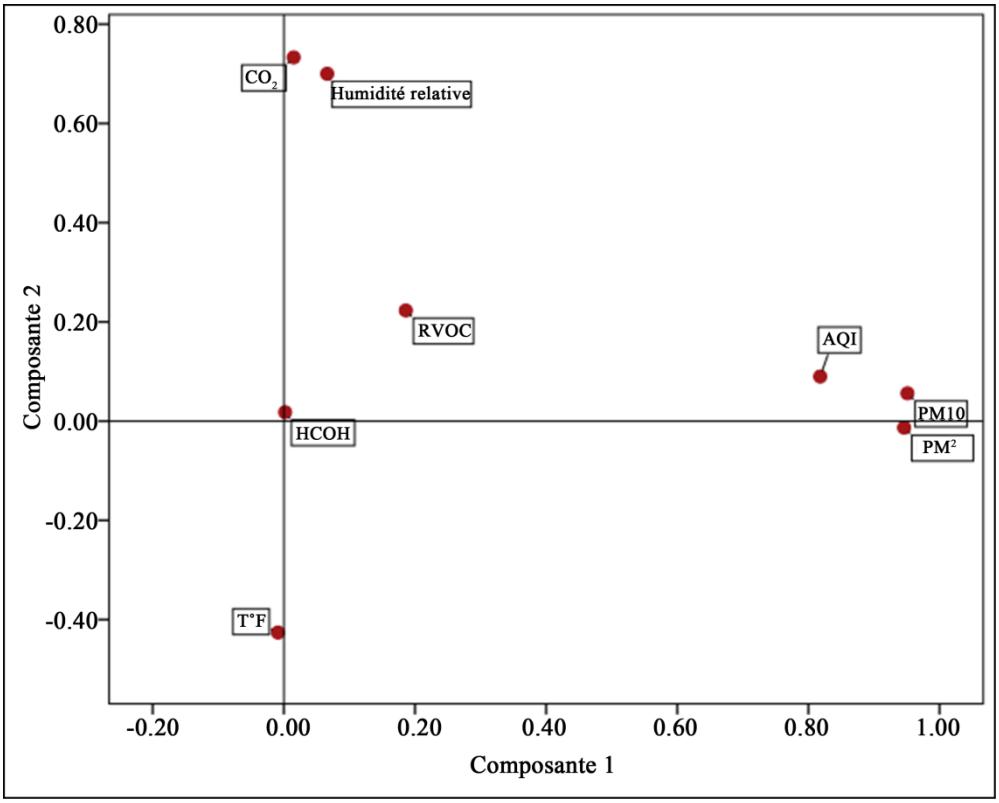

Figure 17. Graphical representation of the F1-F2 factor map.

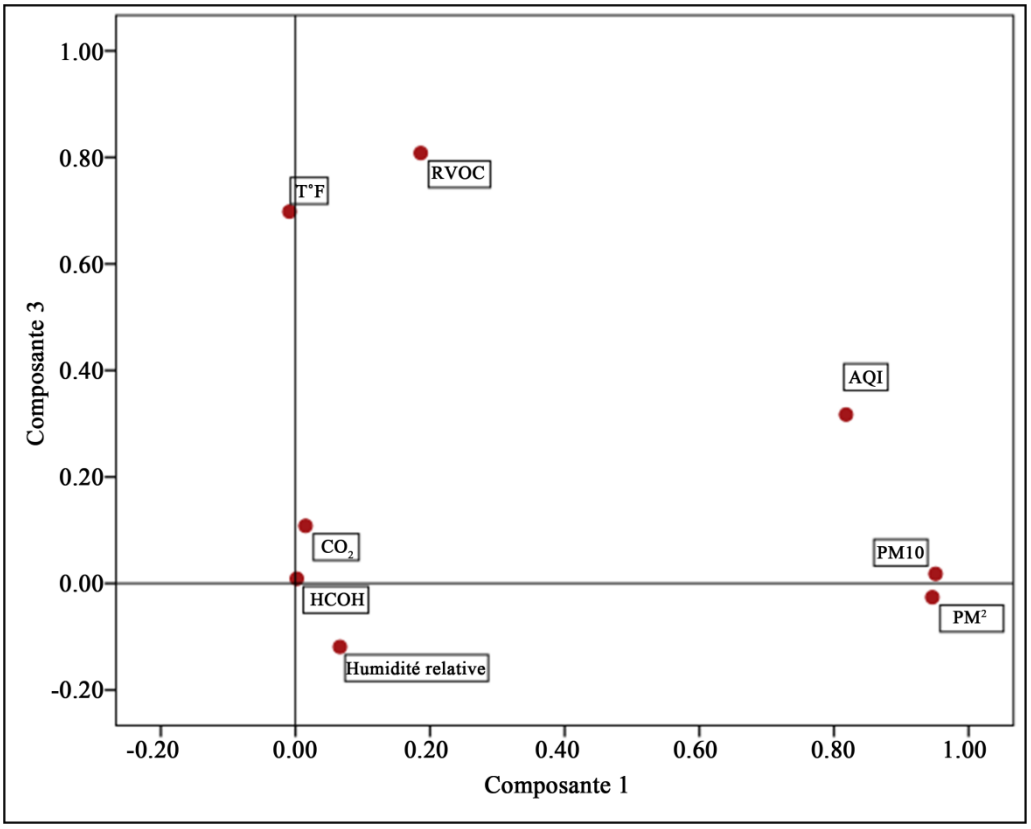

Figure 18. Graphical representation of the F1-F3 factor map.

Figure 20 shows the graphical representation of the factorial map F1-F2 and F1-F3.

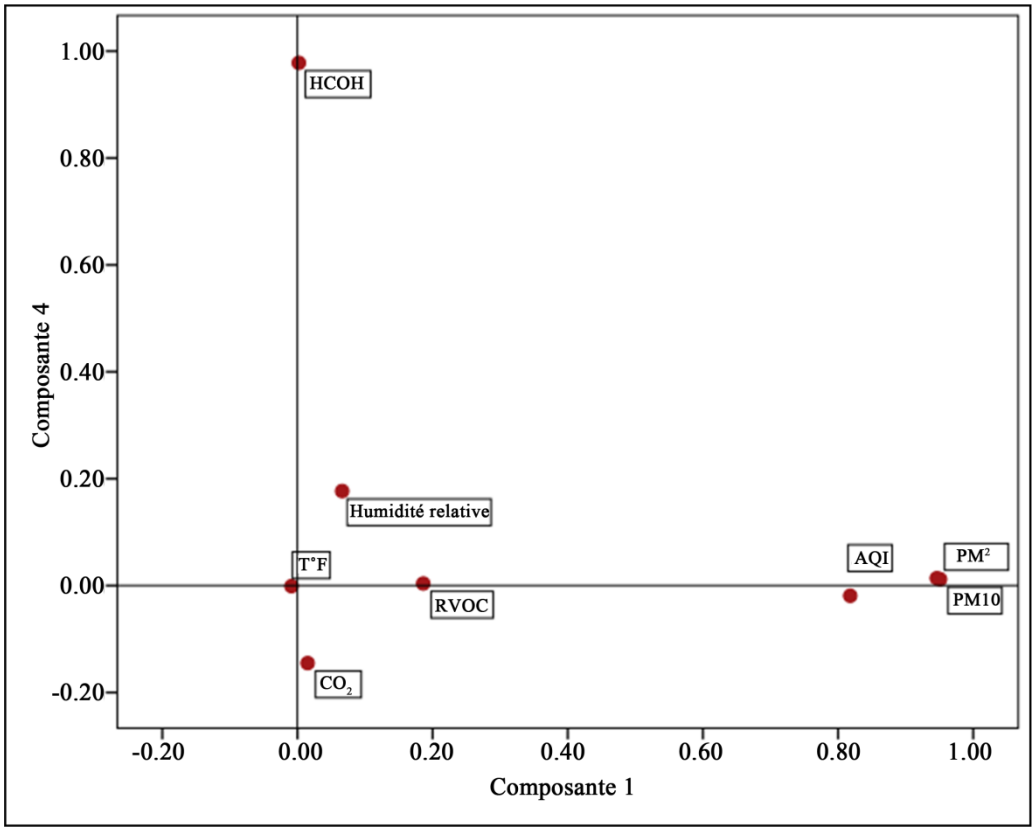

Figure 19. Graphical representation of the F1-F4 factor map.

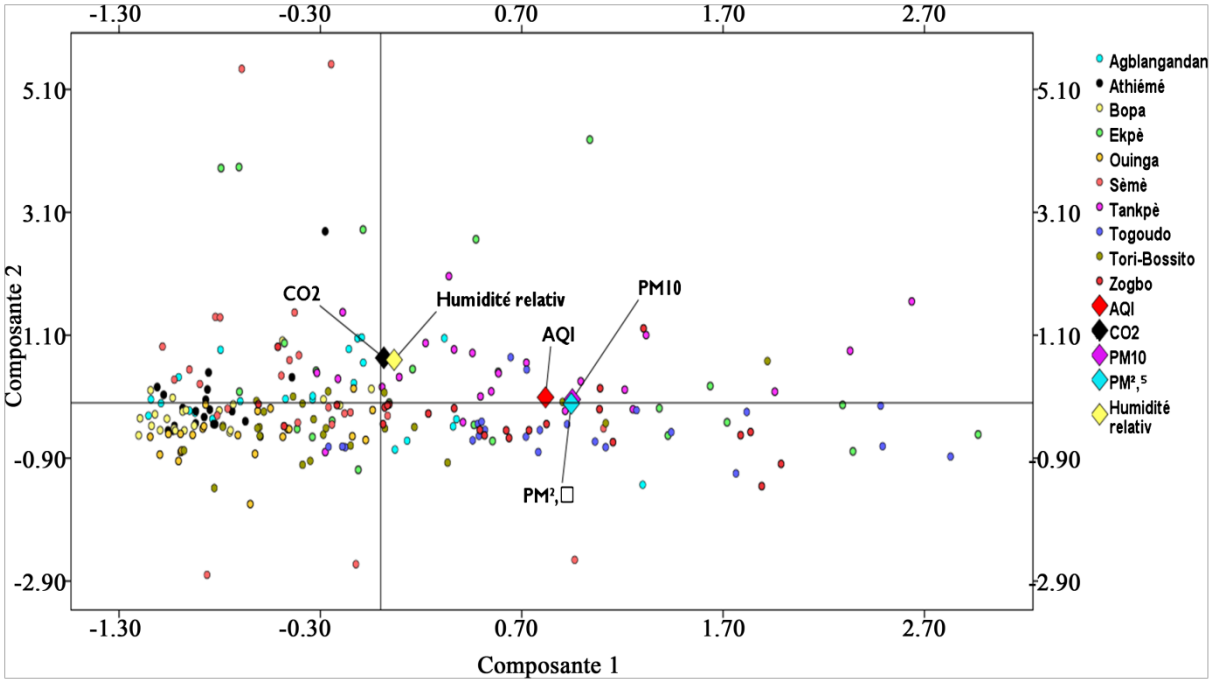

Figure 20. Graphical representation of the factorial map F1-F2 and F1-F3.

The analysis of Figure 20 shows two groups of points, namely those located to the left of the ordinate axis and grouped around the abscissa axis. These are the points Aglangandan, Zogbo, Athiémé, Bopa, Ouiga characterized by a good Air Quality Index. All other points located to the right of the y-axis and grouped around the x-axis are characterized by moderate to severe Ambient Air Quality Indices. These are Sèmè, Ekpè, Tankpè, Togoudon Tori-Bossito, Carrefour Etoile rouge, Carrefour Toyota and crossroads after friendship stadium. At these last points, the quality of ambient air is marked by high levels of particulate matter, especially $PM_{2.5}$, TCOV, sometimes HCHO and CO_2. Particulate matter and TVOCs are two classes of air pollutants most harmful to human health.

4. Discussion

From our results, it appears that air pollution levels vary from 400 to 1444 ppm with an average of 486.80 ± 184.3 ppm and a %CV = 37.86 for carbon dioxide CO_2. At the level of Total Volatile Organic Compounds (TCOV), the daily contents vary from 0.01 to 6.91 mg/m^3 with a daily average of 0.36 ± 0.65 mg/m^3 and a %CV = 181.4. Aldehydes vary from 0.005 to 3 mg/m^3 with an average of 0.05 ± 0.17 mg/m^3 and a %CV = 320.38. Regarding particulate matter with diameters less than or equal to 2.5 µm ($PM_{2.5}$), pollution levels vary between 5 and 173.8 µg/m^3 with an average of 21.5 ± 17.62 µg/m^3 and a %CV = 82. On the other hand, for PM_{10}, the contents vary from 5 to 449.6 µg/m^3 with an average of 28.17 ± 31.74 µg/m^3 and a %CV = 112.67. The Air Quality Index (AQI) ranges from 0.3 to 243 with a mean of 39 ± 33.16 and a %CV of 85.38. Concerning the spatial distribution of the pollutants monitored, only particulate matter, TCOV and AQI make it possible to model pollution based on the distances which separate the sampling points. The most polluted city is the city of Cotonou, especially by particulate matter, especially $PM_{2.5}$ and TCOV. Other authors recorded $PM_{2.5}$ contents of around 335.1 µg/m^3 in 2016 in Cotonou [14] and 175.3 µg/m^3 in Cotonou in 2017 [15]. The $PM_{2.5}$ contamination levels recorded by [15] are similar to our results and allow us to conclude that the evolution of $PM_{2.5}$ pollution in Cotonou remained stagnant from 2017 to 2023. However, during During this same period, the automobile fleet experienced an evolution. The data from [14], [15] and our results highlight the effectiveness of the different policies to combat air pollution in the large cities of Benin, implemented by the different successive governments at the head of the Beninese state. [16] by working in two African cities namely Abidjan and Cotonou on other atmospheric pollutants in addition to ours such as (NO_2, SO_2, NH_3, HNO_3, O_3) showed a weak seasonality of concentrations and the majority pollutants on all sites are NH_3 and NO_2 with higher concentrations. However, the sites identified by the author in the city of Cotonou are the major intersections of road arteries. In other words, the major intersections of the city of Cotonou are under the influence of significant atmospheric pollution according to the study and this pollution is generalized throughout the city with regard to NH_3 and NO_2. This is in agreement with the present study

which revealed the influence of the city of Cotonou, especially the major intersections, by $PM_{2.5}$ and TCOV. This trend is also reported by [4] who showed that the city of Kinshasa in the Democratic Congo is also polluted by NO_2 and CO. [17], while working in the city of Tunis in Tunisia noticed high concentrations of ozone in the study area, and their distribution opposite to that of concentrations of nitrogen oxides and sulfur dioxide, even if the values of the latter do not exceed the standards (respectively. The correlation matrix as well as the PCA made it possible to note a strong correlation between ozone, temperature and the intensity of solar radiation, on the one hand, and the relative humidity of the air and the concentration of nitrogen monoxide, on the other hand, these two groups being anti-correlated. The concentrations of nitrogen dioxide appear here to be independent of photochemical phenomena and very poorly correlated to other parameters. In our study we also noted that among the pollutants monitored there were two classes: pollutants characterizing severe pollution such as TVOC and $PM_{2.5}$ and those whose levels of presence in the atmosphere were not threatening for target groups such as newborns, the elderly and those who suffered from respiratory pathologies.

5. Conclusion

The analysis of the different distribution maps shows a standard deviation ellipse oriented in the East-West direction, suggesting an orientation of the spatial distribution of the contents of the atmospheric pollution monitoring parameters in the study area. This observation led to the statistical tests of Moran, General G and sometimes, if the need arises, to the calculations of the Anselin-Moran and Getis and Ord indices to confirm or refute not only the spatial distribution but also to highlight the zones of similarity/dissimilarity and zones of high and low concentrations. Of the 13 monitoring sites and the 8 parameters chosen to determine the ambient air quality in southern Benin, only three parameters present spatial autocorrelation leading to predictions of ambient air quality over the entire study area in based on the distance between the points. These 3 parameters are $PM_{2.5}$, PM_{10} and the ambient air quality index (AQI). The localities affected by atmospheric pollution in South Benin are located in the south-western part of Benin headed by the city of Cotonou which is heavily polluted by CO_2, Total Volatile Organic Compounds (TCOV), PM_{10} and especially $PM_{2.5}$. These levels of pollution in the city of Cotonou are likely to impact sensitive people such as the elderly, newborns and patients with acute and chronic respiratory illnesses.

Conflicts of Interest

The authors declare no conflicts of interest regarding the publication of this paper.

References

[1] Cachon, F.B.A. (2013) Study of Air Pollution in Sub-Saharan Africa: Case of Coto-

nou (Benin): Physicochemical Characterization of Particulate Matter of Urban Origin and Toxicological Impact on Human Bronchial Epithelial Cells (BEAS-2B) Cultured *in vitro*. Ph.D. Thesis, Université du Littoral Côte d'Opale, University of Abomey-Calavi, Benin.

[2] Rodriguez, Y.P., Holy, H.M., Alexis, V.S., Ruffin, B.N., Rosine, M. and Jules, A.K. (2022) Monitoring Air Quality in the City of Kinshasa by Mobile Measurements of Atmospheric NO_2 at Different Geographical Points. *Environment, Engineering & Development*, **86**, 13-21. https://doi.org/10.46298/eid.2022.8379

[3] Ndong, A. (2019) Outdoor and Indoor Air Pollution in Dakar (Senegal): Characterization of Pollution, Toxicological Impact and Epidemiological Assessment of Health Effects. Toxicology. Ph.D. Thesis, The Universities of Littoral Côte d'Opale, Cheikh Anta Diop in Dakar, Dakar, 197 pp.

[4] Newell, K., Kartsonaki, C., Lam, K.B.H. and Kurmi, O.P. (2017) Cardiorespiratory Health Effects of Particulate Ambient Air Pollution Exposure in Low-Income and Middle-Income Countries: A Systematic Review and Meta-Analysis, *The Lancet Planetary Health*, **1**, e368-e380. https://doi.org/10.1016/S2542-5196(17)30166-3

[5] Suk, W.A., Ahanchian, H., Asante, K.A., Carpenter, D.O., Diaz-Barriga, F., Ha, E.-H., Huo, X., King, M., Ruchirawat, M. and Da Silva, E.R. (2016) Environmental Pollution: An Under-Recognized Threat to Children's Health, Especially in Low- and Middle-Income Countries, *Environmental Health Perspectives*, **124**, A41-A45. https://doi.org/10.1289/ehp.1510517

[6] WHO (2016) Ambient Air Pollution: A Global Assessment of Exposure and Burden of Disease. http://apps.who.int/iris/bitstream/10665/250141/1/9789241511353-eng.pdf?ua=1

[7] African Consulting Company (ACC) (2015) Evaluation and Updating of the Sub-Program to Combat Air Pollution in the Large Cities of Benin. Expert Report, 197 pages.

[8] Houénou, P. (2017) Feasibility Study and Implementation of the Project to Create Environmental Observation in Benin (PCOEB). Master Memory, 93 pages.

[9] Gbaguidi, M. (2012) Evaluation and Updating of the Sub-Program to Combat Air Pollution in the Large Cities of Benin. Expert Report, 180 pages.

[10] Dunn, O. (1961) Multiple Comparisons among Means. *Journal of the American Statistical Association*, **56**, 52-64. https://doi.org/10.1080/01621459.1961.10482090

[11] Moran, P.A.P. (1950) Notes on Continuous Stochastic Phenomena. *Biometrika*, **37**, 17-23. https://doi.org/10.1093/biomet/37.1-2.17

[12] Getis, A. and Ord, J.K. (1992) The Analysis of Spatial Association by Use of Distance Statistics. *Geographical Analysis*, **24**, 189-206. https://doi.org/10.1111/j.1538-4632.1992.tb00261.x

[13] Anselin, L. and Getis, A. (1992) Spatial Statistical Analysis and Geographic Information Systems. *The Annals of Regional Science*, **26**, 19-33. https://doi.org/10.1007/BF01581478

[14] Xu, H., Léon, J.-F., Liousse, C., Guinot, B., Yoboué, V., Akpo, A.B., Adon, J., Ho, K.F., Ho, S.S.H., Li, L., Gardrat, E., Shen, Z. and Cao, J. (2019) Personal Exposure to $PM_{2.5}$ Emitted from Typical Anthropogenic Sources in Southern West Africa: Chemical Characteristics and Associated Health Risks. *Atmospheric Chemistry and Physics*, **19**, 6637-6657. https://doi.org/10.5194/acp-19-6637-2019

[15] Adon, A.J, Liousse, C., Doumbia, E.T., Baeza-Squiban, A., Cachier, H., Léon, J.F., Yoboué, V., Akpo, A.B., Galy-Lacaux, C., Guinot, B., Zouiten, C., Xu, H., Gardrat, E. and Keita, S. (2020) Physico-Chemical Characterization of Urban Aerosols from

Specific Combustion Sources in West Africa at Abidjan in Côte d'Ivoire and Cotonou in Benin in the Frame of the DACCIWA Program. *Atmospheric Chemistry and Physics*, **20**, 5327-5354. https://doi.org/10.5194/acp-20-5327-2020

[16] Bahino, J. (2018) Analysis of Air Quality in Urban Areas in Africa: Characterization of Gas Pollution of Chemical Species NO_2, SO_2, HNO_3, NH_3 and O_3 in Abidjan and Cotonou. Ph.D. Thesis, Felix Houphouët-Boigny University, Abidjan.

[17] Kchih, H.M. and Cherif, S. (2015) Spatial Distribution of O_3, NO_x and SO_2 and Evaluation of Tropospheric Interactions in Tunis (Tunisia). *International Conference in Integrated Management of Environment*, Yassmin Hammamet, September 2014.